

A new method of guidance control for autonomous rendezvous in a cluttered space environment

Nicholas Martinson¹ and Josue D. Munoz²
University of Florida, Gainesville, Florida, 32611

Dr. Gloria J. Wiens³
University of Florida, Gainesville, Florida, 32611, USA

[Abstract] This paper addresses a new concept of autonomous guidance for close proximity operations in space. A potential function is developed with the intent that a minimum occurs at a desired relative position. A control law is then used to account for the dynamic effects and ensure the path generated is obstacle free. CW maneuvers are used to traverse solutions provided from the guidance algorithm. Trajectories are shown for a variety of situations in which a completely autonomous spacecraft can rendezvous with a cooperative satellite in an unspecified amount of time. A comparison is made between the new algorithm and traditional APFG methods by examining the total impulse thrusts and time of flight. It is shown that the new algorithm is more fuel efficient and has a shorter time of flight than traditional APFG methods.

Nomenclature

ESR	=	Expert Space Robot
RSO	=	Resident Space Object
CW	=	Clohessy-Wiltshire
APFG	=	Artificial Potential Function Guidance
RHC	=	Receding Horizon Control
TOF	=	time of flight
μ	=	gravitational parameter
n	=	mean motion
t^*	=	time of flight
f	=	specific force applied from thrust
\underline{r}	=	relative position vector
\underline{r}_0	=	initial relative position vector
$\underline{\dot{r}}$	=	relative velocity vector
$\underline{\dot{r}}_0$	=	initial relative velocity vector
$\Delta \underline{v}$	=	impulse vector
$\underline{\dot{r}}_0^-$	=	initial relative velocity vector before impulse
$\underline{\ddot{r}}$	=	relative acceleration vector
$\underline{\hat{r}}$	=	relative position of obstacle
$\underline{\Phi}(t, t_0)$	=	state transition matrix
\underline{A}	=	state matrix
\underline{B}	=	input vector

¹ Graduate Student, Mechanical and Aerospace Engineering, ufmartsn@ufl.edu, AIAA Student Member

² Graduate Student, Mechanical and Aerospace Engineering, jdm03@ufl.edu, AIAA Student Member

³ Associate Professor, Mechanical and Aerospace Engineering, gwiens@ufl.edu

ϕ	=	potential
\underline{P}	=	shape matrix for attractive potential
\underline{M}	=	shape matrix for repulsive potential
Ψ	=	height parameter for Gaussian repulsive potential
σ	=	width parameter for Gaussian repulsive potential

I. Introduction

Autonomous rendezvous and servicing of space assets has been considered for many years as a means to extend space systems' lifetimes and reduce space mission costs. There are many missions for which proximity and non-proximity operations are being researched such as DARPA's Orbital Express Vehicle¹², DARPA's SUMO robot¹³, the European Space Agency's ATV (Automated Transfer Vehicle)¹⁴, Daimler-Chrysler's ISS Inspector¹⁵, NASA's Personal Satellite Assistant¹⁶, XSS 11¹⁷, ETS VII²⁰, and SPHERES¹⁹. While, autonomous trajectory planning and obstacle avoidance for nonholonomic systems is a well-studied topic^{1,10}, methods for holonomic systems are not as well-studied; particularly space systems because of monetary cost.

The two areas for improvement in which this paper addresses is the need to keep fuel usage and computational load to a minimum. An approach by Ref. 6-8 uses Artificial Potential Function Guidance (APFG) algorithms where both of these areas are addressed. APFG methods are attractive because a cost function is explicitly designed to have a minimum at the goal and for which its solution lends well to a Steepest Descent approach which is computationally efficient. The drawbacks to these algorithms are that they are not optimal with respect to fuel usage and they may contain local minima¹. In addition, the inputs provided would be appropriate if the resulting trajectories were linear, however, only nonlinear trajectories are feasible in space⁸. Another drawback of these algorithms is they do not gracefully avoid obstacles, which can be seen as a problem from both a fuel usage and local minima standpoint¹.

Other guidance algorithms have been developed from an optimal control standpoint [9,21]. This method has the advantage that fuel use is minimized and that local minima are avoided because the solution is global. The approach taken by Ref. 9 develops a cost function that includes important physical parameters such as fuel use, time of flight (TOF), control effort, and obstacle clearance distance. While the cost function uses the translational and rotational dynamic equations, both the obstacles' and target's motion must be prescribed for the entire TOF in order for the trajectory to be valid. The algorithm also required good initial guesses in order for the algorithm to converge¹¹. It should also be noted that these solutions are often computationally intensive and not suitable for real-time implementation. The approach taken by Ref. 21 shows that fast robust codes are available for autonomous space systems in a highly cluttered environment. This control scheme, however, is not suitable for real-time application because of the simplified nature of the assumed environment. The assumptions are that the obstacles are static, and there is no attempt to deal with model/plant mismatch. Also, the nature of the optimization leads to the problem that the resulting trajectory between time steps may not be feasible. This is particularly problematic because the solution often tends to be close to constraint regions because the cost function is the total fuel consumption.

The method discussed in this paper shows how control inputs derived from an artificially generated potential function can be solved for, that lead to lower fuel consumption than by the previous method of Steepest Descent. This is used purely for obstacle avoidance whereas fuel efficient Clohessy-Wiltshire (CW) maneuvers can be used to traverse solutions where obstacles are not present. This method is then directly compared to APFG methods which show that the new guidance control algorithm is more fuel efficient with shorter times of flight and still accomplishes real-time guidance control in the presence of obstacles. It is assumed that sensor information is used to determine position and velocity of obstacles and so their motion is not known a priori. By using this method, the Lyapunov function with the control law should be able to account for moving obstacles as well as unmodeled disturbances and sensor noise. This method has the same advantages as APFG in that there is no specified amount of time for rendezvous and that it is computationally efficient. However, these results suffer because the total fuel usage is not optimal, local minima are not eliminated, and obstacle geometry is not accurately represented.

II. System Dynamics

A. Relative Motion

The objective of this problem is for a chaser vehicle denoted as Expert Space Robot (ESR) to rendezvous with a target vehicle denoted as Resident Space Object (RSO) in a space environment. When considering relative motion between the center of mass of two bodies in close range orbiting the Earth, it is customary to use the CW Equations

(also known as Hill's Equations). The underpinning assumptions are that the target body is traveling in a circular orbit and the two bodies are relatively close together.

Using the assumptions previously stated, the governing equation for relative motion can be obtained and is linear as shown in Eq. (1) with its basis as the RSW frame (defined in Figure 1)^{2,3}:

$$\begin{aligned} \ddot{x} - 2n\dot{y} - 3n^2x &= f_x \\ \ddot{y} + 2n\dot{x} &= f_y \\ \ddot{z} + n^2z &= f_z \end{aligned} \quad (1)$$

Here x, y, z are the coordinates of the relative position of the ESR, n is the mean motion of the RSO, and f_x, f_y, f_z is the specific force applied by the thrusters of the ESR in the x, y, z directions respectively.

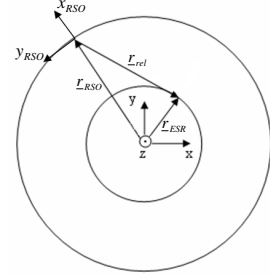


Figure 1. RSW frame defined. x_{RSO} is the R-bar direction and y_{RSO} is the V-bar direction.

Equation (1) can be written in state space form as shown in Eqs. (2)

$$\dot{\underline{x}} = \underline{A}\underline{x} + \underline{B}u, \underline{x}(0) = \underline{x}_0 \quad (2)$$

where \underline{x}_0 is the column vector containing the initial positions x_0, y_0, z_0 and the initial velocities $\dot{x}_0, \dot{y}_0, \dot{z}_0$. The homogenous solution to this equation can be obtained analytically² and is shown in Eqs. (3,4)

$$\begin{aligned} \begin{Bmatrix} \underline{r}(t) \\ \underline{\dot{r}}(t) \end{Bmatrix} &= \underline{\Phi}(t, t_0) \begin{Bmatrix} \underline{r}_0 \\ \underline{\dot{r}}_0 \end{Bmatrix} \quad (3) \\ \begin{Bmatrix} x \\ y \\ z \\ \dot{x} \\ \dot{y} \\ \dot{z} \end{Bmatrix} &= \begin{bmatrix} 4-3\cos(nt) & 0 & 0 & \frac{\sin(nt)}{n} & \frac{2}{n}(1-\cos(nt)) & 0 \\ 6(\sin(nt)-nt) & 1 & 0 & -\frac{2}{n}(1-\cos(nt)) & \frac{4\sin(nt)-3nt}{n} & 0 \\ 0 & 0 & \cos(nt) & 0 & 0 & \frac{\sin(nt)}{n} \\ 3n\sin(nt) & 0 & 0 & \cos(nt) & 2\sin(nt) & 0 \\ -6n(1-\cos(nt)) & 0 & 0 & -2\sin(nt) & 4\cos(nt)-3 & 0 \\ 0 & 0 & -n\sin(nt) & 0 & 0 & \cos(nt) \end{bmatrix} \begin{Bmatrix} x_0 \\ y_0 \\ z_0 \\ \dot{x}_0 \\ \dot{y}_0 \\ \dot{z}_0 \end{Bmatrix} \quad (4) \end{aligned}$$

where $\underline{\Phi}(t, t_0)$ is the state transition matrix. It will be shown that one can use the homogeneous solution to model the motion of the ESR by simply augmenting the initial velocities with the impulsive inputs.

B. Impulsive Response

Recall that the governing equations for the system in state space form are given by Eq. (2). The impulse response of the system is then shown in Eq. (5) where \underline{x} represents the states (i.e. position and velocity) and $u(t)$ is an ideal impulse.

$$\underline{x}(t) = e^{\underline{A}t} [\underline{x}_0 + \underline{B}] = \underline{\Phi}(t, t_0) [\underline{x}_0 + \underline{B}] \quad (5)$$

Thus, it is important to note that for an impulse response, the initial conditions \underline{x}_0 were augmented by the input vector \underline{B} . This is convenient since when performing a CW maneuver one will be using this property to derive the required impulse for a CW maneuver.

C. CW Maneuvers

A CW maneuver can be defined as the single impulse input that would be required to reach a prescribed position. The impulse input required for a CW maneuver can be derived from the homogenous solution, Eq. (3,4), to the CW Equations.

$$\begin{Bmatrix} \underline{r}(t) \\ \dot{\underline{r}}(t) \end{Bmatrix} = \underbrace{\underline{\Phi}(t, t_0)}_{6 \times 6} \begin{Bmatrix} \underline{r}_0 \\ \dot{\underline{r}}_0 \end{Bmatrix} = \begin{bmatrix} \underbrace{\underline{\Phi}_{1,1}(t, t_0)}_{3 \times 3} & \underbrace{\underline{\Phi}_{1,2}(t, t_0)}_{3 \times 3} \\ \underbrace{\underline{\Phi}_{2,1}(t, t_0)}_{3 \times 3} & \underbrace{\underline{\Phi}_{2,2}(t, t_0)}_{3 \times 3} \end{bmatrix} \begin{Bmatrix} \underline{r}_0 \\ \dot{\underline{r}}_0 \end{Bmatrix} \quad (6)$$

From the first row of Eq. (6), one can determine relative position as strictly a function of time. Thus, if one chooses a TOF and considers the initial velocity to be the initial velocity before the impulse plus the impulse vector, then one can solve for the impulse vector for the desired relative position.

$$\underline{r}(t^*) = \underline{\Phi}_{1,1}(t^*, t_0) \underline{r}_0 + \underline{\Phi}_{1,2}(t^*, t_0) (\dot{\underline{r}}_0^- + \Delta \underline{v}_i) \quad (7)$$

$$\Delta \underline{v}_i = \underline{\Phi}_{1,2}^{-1}(t^*, t_0) (\underline{r}(t^*) - \underline{\Phi}_{1,1}(t^*, t_0) \underline{r}_0) - \dot{\underline{r}}_0^- \quad (8)$$

For Eqs. (7,8), t^* is the TOF, $\underline{r}(t^*)$ is the prescribed destination, and $\underline{r}_0, \dot{\underline{r}}_0^-$ are the position and velocity before the impulse.

The same can be done to calculate the impulsive input required for zero relative velocity by looking at the second row of Eq (6). The resulting CW maneuver is defined in Eq. (9)

$$\Delta \underline{v}_f = -\underline{\Phi}_{2,1}(t^*, t_0) \underline{r}_0 - \underline{\Phi}_{2,2}(t^*, t_0) (\dot{\underline{r}}_0^- + \Delta \underline{v}_i) \quad (9)$$

III. Artificial Potential Function Guidance

The solution to the CW equations can be used to develop the APFG methodology. In order to ensure convergence, the APF's will be defined as Lyapunov functions which have the following properties:

$$\left. \begin{array}{l} \phi(\underline{r}, t) > 0 \quad \forall \quad \underline{r} \neq \underline{0} \\ \phi(\underline{r}, t) = 0 \quad \text{for} \quad \underline{r} = \underline{0} \end{array} \right\} \text{positive definite} \quad (10)$$

$$\dot{\phi}(\underline{r}, \dot{\underline{r}}, t) < 0 \quad \forall \quad \underline{r}, \dot{\underline{r}} \rightarrow \underline{0} \quad \text{negative definite} \quad (11)$$

The potential function developed must have the property that there is a minimum at the goal (attractive potential) and high regions of potential at the obstacles' position (repulsive potential). The total potential function used will be defined as the sum of the attractive and repulsive potentials.

$$\phi = \phi_{att} + \phi_{rep} \quad (12)$$

The forms used for the potential functions for both the attractive and repulsive parts are defined below.

A. Attractive Potential

$$\phi_{att}(\underline{r}, t) = \underline{r}^T \underline{P} \underline{r} \quad (13)$$

In Eq. (13) the parameter \underline{P} is a positive definite matrix that will be used with the attractive potential to give an ellipsoidal projection of the potential in the configuration space.

B. Repulsive Potential

$$\phi_{rep}(\underline{r}, t) = \underline{r}^T \underline{r} \sum_i \Psi_i \exp \left(- \frac{(\underline{r} - \hat{\underline{r}}_i)^T \underline{M}_i (\underline{r} - \hat{\underline{r}}_i)}{\sigma_i} \right) \quad (14)$$

In Eq. (14) $\hat{\underline{r}}_i$ is the position of the obstacle relative to the RSO, the parameters Ψ, σ define height and width of the potential function respectively, and \underline{M}_i is a positive definite matrix that will give an ellipsoidal projection of the repulsive potential onto the configuration space. It should be noted that the relative motion of the obstacles is not considered in this problem.

C. Control Law

The following control law is used to ensure that the solution $\underline{r}(t)$ remains bounded and that convergence is guaranteed. By imposing this control law we are ensuring that $\dot{\phi}(\underline{r}, \dot{\underline{r}}, t) < 0$ ^{7,8}.

$$\underline{f}_{\text{thrust}} = \begin{cases} 0 & \text{if } \dot{\phi}(\underline{r}, \dot{\underline{r}}, t) < 0 \\ \delta(t) \Delta \underline{v} & \text{if } \dot{\phi}(\underline{r}, \dot{\underline{r}}, t) \geq 0 \end{cases} \quad (15)$$

$$\dot{\underline{r}}^- + \Delta \underline{v} = -k \nabla \phi \quad (16)$$

In Eq. (15), $\delta(t)$ is an ideal impulse and $\Delta \underline{v}$ is determined by Eq. (16). In Eq. (16), k is simply a proportional gain to try and attain realistic constraints on thruster actuation.

IV. New Guidance Algorithm

A. Theory

The idea is that we have a switching controller in which one part contains a control to obtain guidance to a terminal region and another for obstacle avoidance. The terminal region constraint uses the solution to Hill's equation with an appropriate TOF to find a low fuel thrust to reach the RSO. Since this part of the control essentially drives the ESR to the RSO we select an appropriate TOF based on the bounds of asymptotic stability from a Lyapunov function form of the attractive potential energy. Obstacles are detected when a Lyapunov function of the form of a repulsive potential energy's derivative reach a threshold. The obstacle avoidance procedure is derived using the conservative potential field of both the attractive and repulsive parts as seen in section III. The obstacle avoidance procedure is implemented by heuristically choosing a TOF that will allow the ESR to move a safe distance away from the obstacle.

B. Algorithm

The first part of the switching controller is the algorithm to derive an appropriate TOF to drive the ESR to the RSO.

1. Guidance control without obstacles

The control here uses the attractive potential function form as a Lyapunov function as seen in Eq. (13). In order to maintain asymptotic stability we solve for a TOF that leads to instability as,

$$\begin{aligned} \dot{\phi}_{\text{att}} = \dot{\underline{r}}^T \underline{r} &= 0 \\ \Rightarrow \left(\underline{\Phi}_{\underline{2},1}(t_0, t_0) \underline{r}_0 + \underline{\Phi}_{\underline{2},2}(t_0, t_0) (\dot{\underline{r}}_0^- + \Delta \underline{v}(t^*)) \right)^T \left(\underline{\Phi}_{\underline{1},1}(t_0, t_0) \underline{r}_0 + \underline{\Phi}_{\underline{1},2}(t_0, t_0) (\dot{\underline{r}}_0^- + \Delta \underline{v}(t^*)) \right) &= 0 \end{aligned} \quad (17)$$

where $\Delta \underline{v}(t^*)$ is a CW maneuver with unknown TOF. Once this TOF has been solved for we can select a smaller TOF that maintains stability as well as maintains low fuel usage (i.e. 95% of t^*). The control input is derived by inputting the new t^* into Eq. (8).

2. Guidance control with obstacles

The second part of the controller is used to provide an obstacle avoidance procedure. A Gaussian function, as seen in Eq. (14), is used to define the obstacles' area of artificial potential. The time rate of change of this function is used to check whether a control action is required to avoid obstacles. If an obstacle is detected, Eqs (18,19) define a control law similar to the control law used for APFG that will determine the impulse required to avoid the obstacles.

$$\underline{f}_{\text{thrust}} = \begin{cases} 0 & \text{if } \dot{\phi}_{\text{rep}}(\underline{r}, \dot{\underline{r}}, t) < \kappa \\ \delta(t) \Delta \underline{v} & \text{if } \dot{\phi}_{\text{rep}}(\underline{r}, \dot{\underline{r}}, t) \geq \kappa \end{cases} \quad (18)$$

$$\dot{\underline{r}}^- + \Delta \underline{v} = -k \nabla \phi \quad (19)$$

Here κ is a threshold for the rate of a change of the repulsive potential and ϕ is the sum of the attractive and repulsive potentials. The constant κ should depend on the parameters Ψ , σ , and \underline{M} that define the repulsive potential. This avoidance procedure is implemented for a step length τ which is chosen as a reasonable time to maneuver away from an obstacle. In this paper, the value chosen for the simulations presented was $\tau = 100$ seconds although a greater or smaller time could be used. It should be noted that the value of $\dot{\phi}_{\text{rep}}(\underline{r}, \dot{\underline{r}}, t)$ is always checked to ensure the path generated is obstacle free. If obstacles are not encountered and the time τ has elapsed since avoiding an obstacle the control switches to guidance with no obstacles as previously discussed.

V. Simulation and Results

A. Guidance without obstacles

The first simulation tested APFG's performance in an obstacle-free environment. Initially, the ESR is 1 km in the positive R-bar and negative V-bar directions. The simulation was terminated once the ESR was within 20 meters of the target as shown by the region depicted by the circle at the origin. Figure 2 shows a plot of the R-bar and V-bar responses, the history of impulse burns, and the trajectory traversed. Setting \underline{P} equal to identity creates a circular projection of the attractive potential onto the orbit plane. A gain $k = 10^{-3} s^{-1}$ was considered appropriate for this problem.

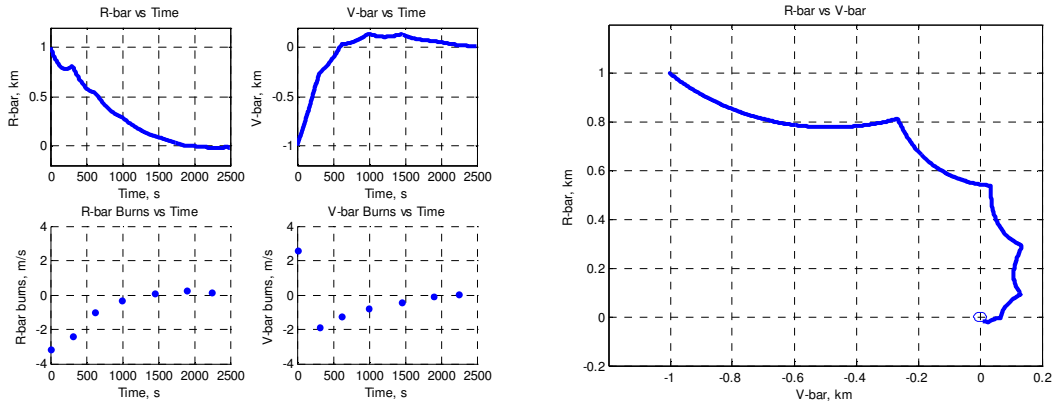


Figure 2. Results for APFG without obstacles. The ESR is initially at the point $(-1, 1)$ and reaches within 20 m of the goal at $(0, 0)$.

The results show that the total amount of impulsive burns required was $\Delta v_{total} = 14.57 m/s$ with a TOF of approximately 2500 seconds.

When using the new guidance control algorithm a single CW maneuver is required to reach the RSO. It is assumed that when the ESR is within 20 meters of the RSO another CW maneuver can be executed in order to drive the relative velocity closer to zero. Figure 3 shows the R-bar and V-bar response obtained as well as the trajectory traversed.

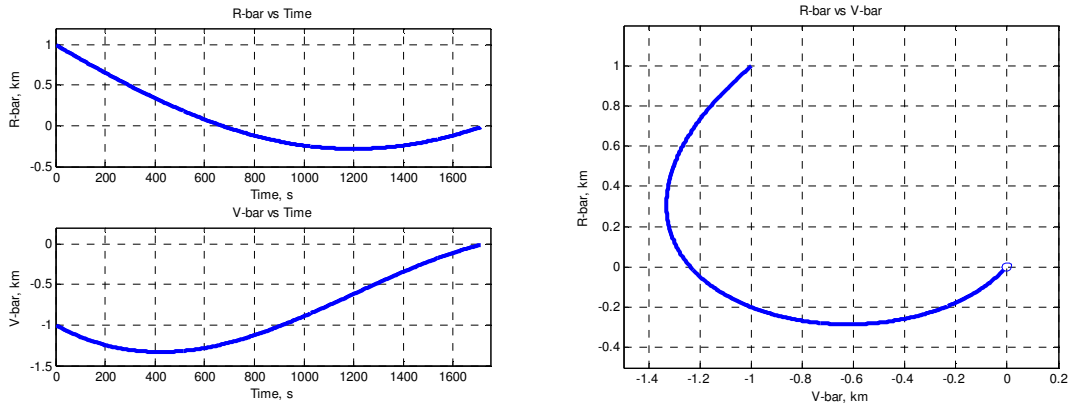


Figure 3. Results for the new algorithm without obstacles. The ESR is initially at the point $(-1, 1)$ and reaches within 20 m of the goal at $(0, 0)$.

The results indicate that the total amount of impulsive burns required was $\Delta v_{total} = 3.98 m/s$ and a TOF of approximately 1700 seconds.

The summary comparison of the results for the unconstrained problem is given in Table 1. The results show that the total impulsive burns required is less for the new algorithm than for the traditional APFG algorithm since the goal was reached using a CW maneuver.

Method	Δv_{total} , m/s	TOF, s	# of Impulses
APFG	14.57	2500	7
New Algorithm	3.98	1700	1

Table 1. Comparison of APFG and new guidance control algorithm for unconstrained problem.

B. Guidance with Obstacles

Simulations were then performed for APFG and the new guidance algorithm in a cluttered environment. \underline{P} was again set to identity as well as for \underline{M} which is in the repulsive potential definitions.

A gain $k = 10^{-3} s^{-1}$ was also considered appropriate for this problem. A random configuration of fifty obstacles was used in order to test which algorithm would have a better performance without having any bias. Three different sizes of obstacles were used as well by randomly choosing between three different values of σ for the repulsive potentials. The value of Ψ was held constant for each different size of obstacle.

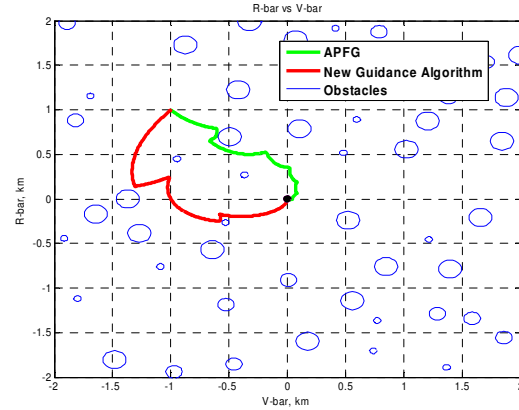


Figure 4. Example of trajectory for APFG and new guidance algorithm in cluttered environment. The ESR is initially at the point (1,-1) and reaches within 20 m of the goal at (0,0).

The obstacles are assumed to all lie on the orbit plane where their positions are in the range $\hat{r}_x, \hat{r}_y \in [-2, 2] km$. An important assumption here is that the position of the obstacles is not known a priori and the position of the objects shown is the position of the obstacle when the ESR detects it.

Fifty simulations were performed for four sets of initial positions since the ESR will behave differently depending on where it is relative to the RSO. Figure 4 shows an example of the trajectories taken by APFG and the new guidance algorithm for an instance where the initial position is $\underline{r}_0 = [1 \ -1 \ 0]^T km$. The initial velocity used for all simulations was $\underline{\dot{r}}_0 = \underline{0} km/s$.

As seen in Figure 5 for the APFG case, it is apparent that normal distributions with different means were encountered for each initial condition. Also, for the new guidance algorithm, it is apparent that skewed distributions with different means were encountered for each initial condition. The means for each initial condition are shown in Table 2, and are apparent in the histogram. In both algorithms, since obstacles were randomly generated, there was an approximately equal probability of

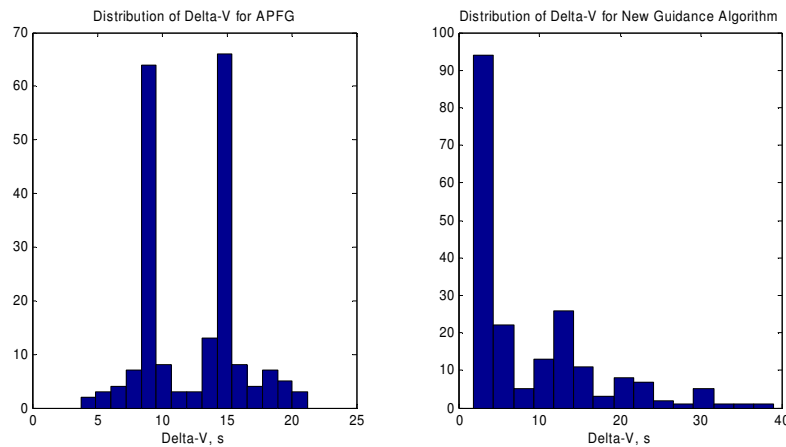


Figure 5. Distribution of Δv_{total} for both APFG and new guidance algorithm.

encountering an obstacle. By visual inspection of the data, it is apparent that both algorithms displayed an approximately equal probability of encountering an obstacle.

Table 2 shows the mean Δv_{total} , mean TOF, and mean number of impulses that resulted for each set of initial conditions. These results show that the new guidance algorithm decreases fuel expenditure, decreases TOF, and decreases total number of impulses when in the presence of obstacles as compared to APFG methods. It can also be noted that in these simulations local minimums for either controller was not encountered.

Method	Mean Δv_{total} , m/s	Mean TOF, s	Mean # of Impulses
APFG	9.11	2787	7.10
New Algorithm	5.30	1680	2.00
<i>Initial Position: $\underline{r}_0 = [1 \ 1 \ 0]^T$ km</i>			
Method	Mean Δv_{total} , m/s	Mean TOF, s	Mean # of Impulses
APFG	15.22	2568	7.34
New Algorithm	11.74	2302	3.59
<i>Initial Position: $\underline{r}_0 = [-1 \ 1 \ 0]^T$ km</i>			
Method	Mean Δv_{total} , m/s	Mean TOF, s	Mean # of Impulses
APFG	9.30	2783	7.04
New Algorithm	4.94	1661	2.60
<i>Initial Position: $\underline{r}_0 = [-1 \ -1 \ 0]^T$ km</i>			
Method	Mean Δv_{total} , m/s	Mean TOF, s	Mean # of Impulses
APFG	15.37	2545	7.59
New Algorithm	13.36	2448	3.84
<i>Initial Position: $\underline{r}_0 = [1 \ -1 \ 0]^T$ km</i>			

Table 2. Comparison of APFG and new guidance algorithm in the presence of obstacles.

VI. Conclusions

This paper demonstrates an improved autonomous guidance controller for space systems over previously known real-time planning algorithms such as APFG. It is the authors' belief that the decreased fuel expenditure with only a slight increase in computational effort due to the minimization algorithm makes this guidance controller a useful tool for path planning missions in space. The increase in computational effort is attributed to calculating the TOF associated with the input for the terminal region constraint. It should be noted that the trajectories generated are still susceptible to local minima and are suboptimal. In order to improve the solution by using APF's it is assumed that the optimal value for the control input should approach the case where no obstacles are present. In this sense it is desired to compute an "early avoidance" scheme so that smaller inputs can be used to avoid obstacles.

References

- ¹Latombe, J.C., *Robot Motion Planning*, Kluwer Academic, Boston, MA, 1991.
- ²Vallado, D.A., *Fundamentals of Astrodynamics and Applications*, Kluwer Academic, Boston, MA, 2001.
- ³Fehse, W., *Automated Rendezvous and Docking of Spacecraft*, Cambridge University Press, 2003.
- ⁴Bate, R.R., *Fundamentals of Astrodynamics*, Dover Publications, Inc., New York, 1971
- ⁵Gill, P.E., *Practical Optimization*, Academic Press, New York, 1981.
- ⁶Tatsch, A.R., "Artificial Potential Function Guidance for Autonomous In-Space Operations", PhD Dissertation, Department of Mechanical and Aerospace Engineering, University of Florida, 2005.
- ⁷Lopez, I and McInnes, C.R., "Autonomous Rendezvous Using Artificial Potential Function Guidance", AIAA Guidance, Control, and Dynamics, 0731-5090, Vol. 18, AIAA, Washington, DC, 1995, pp. 237-241
- ⁸McInnes, C.R., "Autonomous Path Planning For On-Orbit Servicing Vehicles", In *Reducing Space Mission Cost*. British Interplanetary Society, April 1999.
- ⁹Henshaw, C.G., "A Variational Technique for Spacecraft Trajectory Planning", PhD Dissertation, Department of Aerospace Engineering, University of Maryland College Park, 2003.

- ¹⁰Ge, S.S., and Y.J. Cui, "Dynamic Motion Planning for Mobile Robots Using Potential Field Method", *Proceedings of the 8th IEEE Mediterranean Conference of Control and Automation*, Vol. 13, Kluwer Academic, Boston, MA, 2002, pp. 207-222.
- ¹¹Henshaw, C.G., "A Unification of Artificial Potential Function Guidance and Optimal Trajectory Planning", In *Proceedings of the 28th AAS Annual Rocky Mountain Guidance and Control Conference*, Breckenridge, CO, pp. 219-234.
- ¹²<http://www.darpa.mil/tto/programs/oe.htm>
- ¹³http://projects.nrl.navy.mil/sumo/whitePapers/SUMOPaperSPIE5419-7_29Mar04_ver2.doc
- ¹⁴http://www.esa.int/SPECIALS/ATV/ESAE021VMOC_0.html
- ¹⁵http://www.boeing.com/news/releases/1997/news_release_971015b.html
- ¹⁶<http://ic.arc.nasa.gov/projects/psa/index.html>
- ¹⁷<http://www.globalsecurity.org/space/systems/xss.htm>
- ¹⁸Hablani, H.B., Tapper, M.L., Dana-Bashian, D.J. "Guidance and Relative Navigation for Autonomous Rendezvous in a Circular Orbit", *AIAA Journal of Guidance, Control, and Dynamics*, vol. 25, no. 3, pp. 553-562.
- ¹⁹Nolet, Simon, Kong, Edmund, Miller, David W. "Autonomous docking algorithm development and experimentation using the SPHERES testbed", *SPIE Defense and Security Symposium*, Orlando FL, 2004.
- ²⁰http://robotics.jaxa.jp/project/ets7-HP/index_e.html
- ²¹Richards, A., Schouwenaars, T., How, J.P., Feron, E. "Spacecraft Trajectory Planning with Avoidance Constraints Using Mixed-Integer Linear Programming", *AIAA Journal of Guidance, Control, and Dynamics*, vol. 25, no. 4, pp. 755-764.